Ecological Indicators 41 (2014) 155–164

Contents lists available at ScienceDirect

Ecological Indicators

journal homepage: www.elsevier.com/locate/ecolind

Simulation of soil nitrogen storage of the typical steppe with the DNDC model: A case study in Inner Mongolia, China

R.H. Li[a,b,c], X.B. Li[a,c,*], G.Q. Li[d], W.Y. Wen[e]

[a] State Key Laboratory of Earth Surface Processes and Resource Ecology, Beijing Normal University, Beijing 100875, China
[b] School of Surveying & Land Information Engineering, Henan Polytechnic University, Jiaozuo 454000, China
[c] College of Resources Science & Technology, Beijing Normal University, Beijing 100875, China
[d] Institute of Geography & Planning, Ludong University, Yantai 264025, China
[e] Institute of wetland research, Chinese Academy of Forestry, Beijing 100090, China

ARTICLE INFO

Article history:
Received 28 July 2013
Received in revised form 9 December 2013
Accepted 30 January 2014

Keywords:
DNDC
Remote sensing
Soil N storage
Steppe
Inner Mongolia

ABSTRACT

Soil nutrient depletion is one of the characteristics of steppe degradation. Soil nitrogen (N) storage is an indicator of ecosystem productivity, and its simulation is necessary to monitor steppe degradation and for recovery measures. The study presents a simulation framework of soil N storage by integrating a denitrification–decomposition (DNDC) ecosystem model-based simulation and multi-source remote sensing data-based inversion. The DNDC model is a key player in the framework, whereas remote sensing prepares the input parameters and verification data. To run a DNDC model spatially, climate, soil, and vegetation databases were built, and land use, slop, grazing, and mowing parameters were formulated by remote sensing inversion. A soil N storage prediction model was established with the maximum of normalized difference vegetation index (NDVI) to provide comparable results with the simulation of soil N storage with the DNDC model. The results indicate that soil N storage declined from east to west throughout the study area. From 1990 to 2011, no change in the spatial distribution of soil N storage was determined, and the spatial heterogeneity of soil N storage decreased with its increase in the low-N area and decrease in the high-N area. A significant correlation ($P < 0.01$) was determined between soil N storage data detected by remote sensing inversion and that simulated with DNDC, and both estimation results of soil N storage matched well. Soil N storage simulated with the DNDC model was more sensitive to soil organic carbon (SOC), bulk density, pH and N fixation index than other parameters, and using the most sensitive factor (MSF) method, the range of annual mean soil N storage was determined to be between 2339.61 and 5484.61 kg ha^{-1}. The variation in regional soil N storage in a typical steppe in Inner Mongolia, China can therefore be simulated using the DNDC model with support from remote sensing.

1. Introduction

Soil N storage is a nutrient source for vegetative growth (Galloway et al., 2004; Krug et al., 2002), especially in a natural steppe ecosystem with low N fixation and N mineralization (Allison et al., 2010). However, in many of the world's semi-arid regions, the steppe ecosystem is currently facing degradation (Verdoodt et al., 2009), which can significantly affect the carbon (C) cycle, regional economy, and climate (Kirschbaum et al., 2008; Qi et al., 2012; Wang et al., 2007; Wang et al., 2011). Soil N storage is a critical indicator of the degradation extent and the recovery potential of steppes. However, estimation of soil N storage in a steppe ecosystem is complicated by the influence of many factors, including biodiversity, grazing, topography, and climate (Wang et al., 2012).

At present, information on soil N storage of steppes is derived mostly from digging soil profiles by field investigations, with the location of sampling points obtained by the satellite-based global positioning system (Ammann et al., 2009; Huang et al., 2007; Liu et al., 2009; Tian et al., 2006; Yang et al., 2007). Ground-based methods are not practical for extensive geographic areas, especially in remote regions (Feng and Zhao, 2011; Veum et al., 2011; Wang and Chen, 2012).

With remotely sensed data, soil N storage can be inferred from the N stress of vegetation, which is an important indicator that can be monitored (Hilker et al., 2012; Ryu et al., 2011). N, phosphorus (P), and water are the main factors limiting the growth of vegetation in the typical steppe of Inner Mongolia, China (Liu et al., 2009). An abundant supply of N can reduce the negative effect of water stress on the growth and physiology of vegetation in steppes in semi-arid regions (Zhou et al., 2011). Yu et al. (2006) also confirmed

* Corresponding author. Tel.: +86 01058807212
E-mail address: xbli@bnu.edu.cn (X.B. Li).

1470-160X/$ – see front matter © 2014 Elsevier Ltd. All rights reserved.
http://dx.doi.org/10.1016/j.ecolind.2014.01.043

that the constraining effect of N on steppe ecosystems in semi-arid regions is greater than that of water and P. Based on the hypothesis that higher soil N storage leads to better vegetation growth, a regression model of soil N storage and $NDVI_{max}$ can be built at the pixel level, and a reversion of soil N storage can be achieved. However, the method takes the steppe ecosystem as a "black box" and neglects influencing factors and interaction among them (Feng and Zhao, 2011). An ecological process model, such as the CENTURY, Hole-in-the Pipe (HIP), and DNDC models, can conveniently interpret the mechanism by which soil N storage changes. However, such models usually need a large number of parameters, especially for the simulation of regional ecological processes. Remote sensing methods can support process-based ecological models for regional simulations by providing regional model parameters and verifying the simulation results with reversion of soil N storage. Integration of processed-based ecological models and remotely sensed data analysis is a promising method for the simulation framework for soil N storage.

On the basis of field and laboratory observations, some process models have been developed, such as the "HIP" model (Firestone and Davidson, 1989), the Carnegie- Ames-Stanford approach (CASA) model (Potter et al., 1993), the CENTURY model (Parton et al., 1987), and the NGAS model (Parton et al., 1996). With these models, the loss of soil N storage as nitric oxide (NO) and nitrous oxide (N_2O) is calculated as a fraction of rates of either soil N mineralization or nitrification without consideration of the kinetics of the relevant biochemical reaction (Li, 2000). The kinetics of production, consumption, and diffusion of NO and N_2O in the sequential reactions may bring about the variation of soil N storage across climate zones, soil types, or ecosystems at different temporal scale. The DNDC model is equipped with detailed biogeochemical processes of N turnover to simulate N dynamics (Li et al., 2006); can simulate and output the daily step variation of different forms of N, such as ammonium (NH_4^+), nitrate (NH_3^-), NO, N_2O, N_2, and microbial nitrogen; and also output annual variation of N pools when a multi-year simulation is conducted. Therefore, when a simulation of soil N storage spans many years, a multi-year variation of soil N storage can be obtained without revising the structure of the original model. In addition, the dynamic soil temperature and moisture are required to run the HIP, Century and NGAS models, and obtaining these parameters through field experiment is laborious at regional scales. The DNDC model can produce dynamic soil temperature and moisture profiles and shifts of aerobic–anaerobic conditions based on climate database (Li et al., 1992). The climate data are relatively easy to obtain from local meteorological stations. This can greatly reduce manpower and the cost of field work. Furthermore, the soil and vegetation data of DNDC can be well combined with GIS technology that provides a good interface for the remote sensing information, and some parameters, such as slope and land use parameters, can conveniently obtained by remote sensing.

The DNDC model was originally developed to simulate N_2O emissions from cropped soils in the US (Li et al., 1992). Later researchers have modified the model to adapt it to other production systems, and the DNDC model has been applied widely to farmland, forest, wetland, and grassland ecosystems (Li et al., 1994, 2005). Many of these modifications have been incorporated into later versions of the DNDC model (Giltrap et al., 2010). The DNDC model is capable of simulating the magnitudes and dynamics of C and N pools with limited modifications (Li et al., 2011). The emissions of NO, N_2O, N_2, and ammonia (NH_3), as well as seasonal variations of NH_4^+, NO_3^-, and N leaching in soil, have been independently simulated by a wide range of studies worldwide during the past two decades (Butterbach-Bahl et al., 2001; Beheydt et al., 2007, 2008; Li et al., 1992; Li et al., 2006; Wang et al., 1997). Recently, at the Inner Mongolia Grassland Ecosystem Research Station, Xu et al. (2003) and Kang et al. (2011) successfully simulated the N_2O flux and C dynamics with the DNDC model. To our knowledge, the use of the DNDC model in simulating soil N storage variation has not been documented at a regional scale, and it still needs to be tested further.

In this paper, with the modified soil and vegetation parameters, the DNDC model, supported by multisource remote sensing data, was used to simulate regional soil N storage dynamic in Inner Mongolia, China. This study aims to validate the applicability of the DNDC model (version 9.5P) in soil N storage simulation in a typical steppe ecosystem to compare the obtained results with the outcome of remote sensing inversion and to analyze the uncertainty of results related to the input parameters.

2. Study area and research methods

2.1. Study area

The study area is located in the central part of the Xilingol League of Inner Mongolia, China, covering a total area of 97,000 km^2 and spanning from 43°2′ to 46°44′ in latitude and from 113°27′ to 119°12′ in longitude; the area includes Abag Banner, Xilin Hot, West Ujimqin Banner, and the majority of East Ujimqin Banner in the administrative division (Fig. 1). Dominated by a semi-arid climate, the region has a mean annual temperature of 2.2 °C (varying between −2.3 and 5.6 °C) and a mean annual rainfall of 270 mm (varying between 200 and 350 mm) (Li et al., 2012a). The lowest and highest mean monthly temperatures occur in January (−15.4 °C–−22.4 °C) and July (18.2 °C–23.4 °C), respectively. The typical steppe is the main ecosystem type, the dominant vegetation includes *Stipa grandis*, *Stipa krylovii*, *Leymus chinensis*, *Cleistogenes squarrosa*, *Artemisia frigida*, *Caragana korshinski*, and *Agropyron cristatum*, and the growing season is from April to August. Approximately 70% of the annual rainfall falls from June to August, which coincides with the occurrence of peak temperatures (Feng and Zhao, 2011). Rainfall gradually decreases from east to west across the region. The study area is mainly composed of zonal soils, such as light chernozem, meadow chestnut, dark chestnut, chestnut, and light chestnut, which is consistent with the transitional characteristic of the climate. Scattered azonal soils also exist, such as aeolian

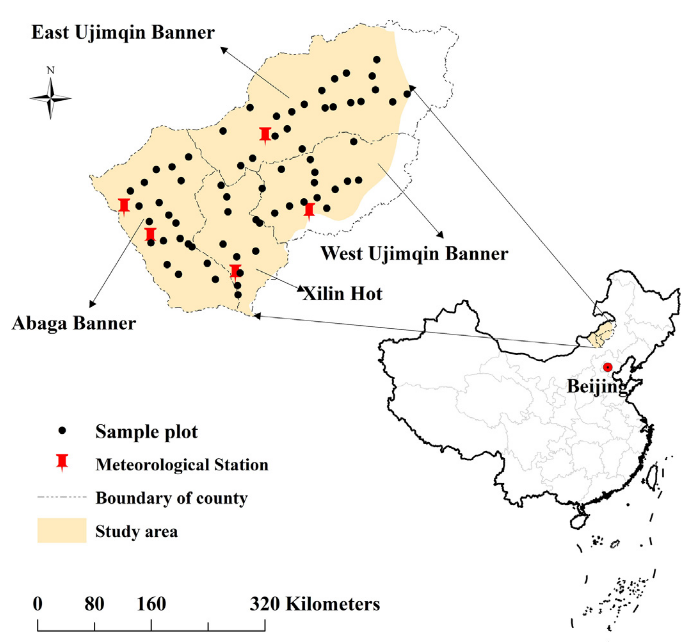

Fig. 1. Location of study area and sample plots.

sandy, bog, fluvo-aquic, salinization chestnut, and regosols. Grazing and mowing are major land use types, and animal husbandry is the main industry in the region.

2.2. DNDC model and its implementation

2.2.1. DNDC model

The DNDC model is a process-based ecosystem model involving in two parts. The first part, which can simulate soil environmental conditions (temperature, moisture, pH, oxidation–reduction potential, and substance concentration), is composed of three submodels, namely, soil and climate, plant growth, and organic matter decomposition. The second part contains three submodels, namely, nitrification, denitrification, and fermentation, which are used to simulate the effect of soil environment on the activity of microorganisms. With these six submodels, DNDC can simulate the variations of C and N pools as well as the emissions of carbon dioxide (CO_2), methane, N_2O (Li et al., 2005; Li et al., 2011), NH_3, NO, and N_2 (Li et al., 2012b) in the vegetation–soil system. More detailed information on the DNDC model can be found in several previous publications (Li et al., 1992, 1994, 2005).

2.2.2. Simulation framework of DNDC supported by remote sensing

To simulate regional soil N storage, the DNDC model needs to divide the region into a series of simulation units and integrate the obtained climate, soil, vegetation, and management measure data into a GIS database (Li et al., 2011). The division of simulation units requires that the ecological driving factors in each unit be relatively consistent. The model takes each simulation unit as a simulation point and uses the simulation result at each point to represent the simulation unit (Li et al., 2011). Based on the information in each simulation unit, simulation unit files are built and read by the DNDC model in batch mode. Therefore, the initial parameters of climate, vegetation and soil set by the model have an important influence on the simulation value in later years. The simulation results are checked by the inversion of remote sensing, which has real-time characteristics. The DNDC model is a key player in the simulation framework, and remote sensing prepares input parameters for the DNDC model and verifies the rationality of simulation results (Fig. 2).

2.2.3. Image data preparation

The images from the Thematic Mapper on NASA's Landsat 5 satellite (30 m resolution) in the growth season of 1990, 1995, 2000, 2005 and 2010 were classified manually to obtain a land use map, which was used to provide assistance in dividing the DNDC simulation units. The advanced spaceborne thermal emission and reflection radiometer global digital elevation model (30 m resolution) was used to generate a slope map. The advanced very-high-resolution radiometer-normalized difference vegetation index (AVHRR-NDVI) data (1000 m resolution; 1990–2008) and the moderate-resolution imaging spectroradiometer (MODIS)-NDVI data (1000 m resolution; 2000–2011) were used to identify the mowing and grazing regions (see Section 2.2.5). The former and latter data were respectively synthesized with the 10 and 16 d maximum and minimum values from June to August. Relevant analysis of AVHRR-NDVI and MODIS-NDVI data from 2000 to 2008 indicated a good correlation between the two data sources at the 0.05 significance level. Approximately 74.24% and 89.31% of the total area of the region had correlation coefficients larger than 0.7 and 0.5, respectively. We assumed that the simultaneous use of the two data sources will only slightly affect the identification of the grazing and mowing regions of each year. We also pre-processed AVHRR-NDVI and MODIS-NDVI data with harmonic analysis of time series (Jakubauskas et al., 2001) to weaken the influence of cloud pollution.

2.2.4. Meteorology, plant, and soil parameters

A meteorological database was built based on the 1990 to 2011 meteorological data provided by five weather stations in Abag Banner, Narenbaolige, West Ujimqin Banner, East Ujimqin Banner, and Xilin Hot (Fig. 1). The meteorological parameters, such as nitrogen content in rainfall and the atmospheric background concentration of NH_3 and CO_2, were determined with the default values of the DNDC model.

A vegetation database was built according to a Chinese vegetation type map at the scale of 1:1,000,000, which was based on a 1980 to 2008 vegetation survey. The vegetation parameters were determined with the dominant vegetation in different steppe types. The dominant vegetation parameters mainly came from the 2011 field quadrat survey and related reference, which are all listed in Table 1.

A soil database was built according to the results of the Xilin Gol League soil survey that was conducted from 1980 to 1987 and was supplemented with a field soil survey in 2011. The main soil parameters are listed in Table 2. Because the salinization chestnut and regosols soils were less than 1% of the total study area, no soil sampling was conducted. The soil parameters of salinization chestnut soil, which was a subclass of the chestnut soil, was set with the

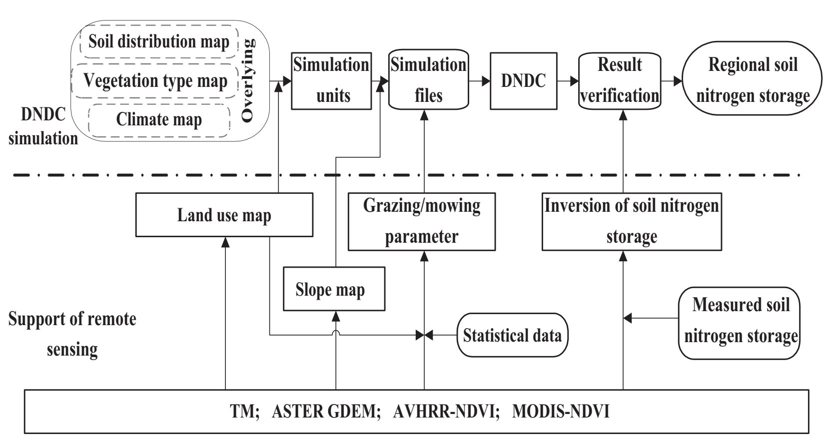

Fig. 2. Simulation framework of soil N storage with the DNDC model supported by remote sensing.

Table 1
Values of input vegetation parameters used in the DNDC model.

Parameters	*Stipa grandis*	*Stipa krylovii*	*Leymus chinensis*	*Cleistogenes squarrosa*	*Artemisia frigida*	*Caragana korshinski*	*Agropyron cristatum*
Maximum biomass production ($kg C ha^{-1} year^{-1}$)[a]	3323.6	1642.2	3536.67	1670	1200.12	2201.55	2578.88
Grain fraction of biomass[a]	0.02	0.04	0.03	0.02	0.06	0.04	0.07
Leaf and stem fraction of biomass[a]	0.55	0.49	0.55	0.5	0.51	0.37	0.57
Root fraction of biomass[a]	0.43	0.47	0.42	0.48	0.43	0.59	0.36
C/N ratio of grain[a]	29.08	28.23	27.78	29.02	17.72	25.26	31.22
C/N ratio of leaf and stem[a]	28.04	26.88	24.73	23.51	23.91	19.45	45.91
C/N ratio of root[a]	48.67	42.99	52.03	59.27	55.39	24.65	44.99
Water requirement ($kg water kg^{-1}$ dry matter)[b]	250	250	250	250	250	250	250
Max_LAI[a]	0.5	0.8	2	2	1	2	1.5
Max_height (m)[a]	0.95	0.7	0.7	0.3	0.6	1.3	0.8
TDD[c]	2500	2500	2500	2500	2500	2500	2500
N fixation index[d]	1.01	1.01	1.01	1.01	1.01	1.01	1.01

[a] Refers to the parameters derived from the field observation.
[b] Refers to the parameters derived from Kang et al. (2011).
[c] Refers to the parameters derived from Chen and Wang (2000).
[d] Refers to the parameters derived from the default values of the DNDC model.

parameters of chestnut soil. The parameters of regosols were set with the default values of sand soil in the DNDC. In addition, the slope parameter was the average of pixels of a unit with the slope image that was extracted from the advanced spaceborne thermal emission and reflection radiometer global digital elevation model (ASTER GDEM) image (30 m resolution).

2.2.5. *Grazing and mowing intensity parameters*

Grazing and mowing are major land use types in the study area and are also the main human driving factors in simulating a steppe ecosystem with the DNDC model. Based on the field survey, the grazing and mowing regions are used separately, i.e., no mowing occurs in the grazing region, and no grazing occurs in the mowing region. The growing season in the study area is from April to August, and the aboveground biomass reaches its maximum in July or August (Bai et al., 2004, 2007; Wu and Loucks, 1992). Little variation is observed in biomass, and the herdsmen mow grass once a year during this period. Given the high correlation between NDVI and land surface biomass ($R^2 = 0.74$) (Jin et al., 2011) in the study area, we calculated the change rate of the aboveground biomass after it was stabilized with Eq. 1. The aboveground biomass has different change rates because of mowing, grazing, and grazing prohibition measure. Thus, we set the change rate of $V = 0.3$ as the threshold value for separating the mowing and grazing regions after several experiments of manual classification combining the spatial distribution of the mowing region obtained in the field survey. The regions with $V > 0.3$, $0 < V \leq 0.3$, and $V = 0$ were taken as the mowing, grazing, and grazing prohibition/non-steppe regions of the year, respectively.

$$V = \begin{cases} \dfrac{(\mathrm{NDVI_{max}} - \mathrm{NDVI_{min}})}{\mathrm{NDVI_{min}}} & (\mathrm{NDVI_{min}} > 0) \\ 0 & (\mathrm{NDVI_{min}} \leq 0) \end{cases}, \tag{1}$$

Table 2
Values of input soil parameters used in the DNDC model and the range of sensitivity parameters

Parameters	Light chernozem	Meadow chestnut	Dark chestnut	Chestnut	Light chestnut	Aeolian sandy	Bog	Fluvo–aquic
Texture	S_loam[a]	S_loam	S_loam	S_loam	S_loam	Sand	S_loam	S_loam
SOC at surface soil (0–5 cm) ($kg C kg^{-1}$)	0.0252	0.0147	0.0198	0.0171	0.0085	0.0038	0.0211	0.0168
	0.0122–0.0446	0.0116–0.038	0.017–0.0227	0.01–0.0224	0.0095-0.0149	0.0003-0.0107	0.0137-0.03	0.0009-0.0347
Clay fraction[b] (0–1)[c]	0.143	0.139	0.086	0.070	0.03	0.03	0.1087	0.0682
Bulk density ($g m^{-3}$)[c]	1.273	1.472	1.393	1.449	1.54	1.53	1.419	1.53
	0.94–1.61	1.38–1.56	1.05–1.80	1.12–1.74	1.39–1.69	1.10–1.77	1.39–1.45	1.24–1.82
pH[c]	7.495	8.635	7.759	7.725	8.24	8.14	7.6	8.28
	7.45–8.47	7.77–9.50	6.20–9.19	6.21–9.26	6.40–10.07	7.30–8.63	7.1–8.16	7.09–9.46
Field capacity (wfps, 0–1)[d]	0.320	0.320	0.320	0.320	0.320	0.150	0.320	0.320
Wilting point (wfps, 0–1)[d]	0.15	0.15	0.15	0.15	0.15	0.10	0.15	0.15
Porosity (0–1)[d]	0.435	0.435	0.435	0.435	0.435	0.395	0.435	0.435
Hydro-conductivity ($m h^{-1}$)[d]	0.208	0.208	0.208	0.208	0.208	1.050	0.208	0.208

[a] S_loam is the abbreviation of sandy loam.
[b] Refers to the parameters derived from Soil Fertilizer Workstation of Xilingol League, 1989.
[c] Refers to the parameters derived from field observation.
[d] Refers to the parameters derived from the default values of the DNDC model; the values with bold font are the change range of the sensitivity parameters.

Table 3
Sensitivity indexes of soil N storage on the main parameters of climate, soil, vegetation, and anthropogenic activity in different vegetation type steppes.

Parameters	*Stipa grandis*	*Leymus chinensis*	*Stipa krylovii*	*Cleistogenes squarrosa*	*Artemisia frigida*	*Caragana korshinski*	*Agropyron cristatum*
Rainfall	0.0024	0.0027	0.0049	0.0048	0.0047	0.0018	−0.0026
Daily temperature	−0.0006	−0.0006	0.0001	0.0002	−0.0005	−0.0001	0.0030
N concentration in Rainfall	0.002	0.002	0.004	0.004	0.004	0.002	0.001
Clay fraction	0.0001	0.00003	0.0005	0.0005	0.0005	0.0002	0.0067
Initial SOC	0.996	0.997	0.995	0.996	0.997	0.997	0.974
Bulk density	0.499	0.499	0.498	0.498	0.499	0.499	0.489
pH	−0.006	−0.006	−0.004	−0.003	−0.005	−0.007	−0.002
N fixation index	0.268	0.269	0.251	0.252	0.183	0.256	0.076
Grazing or mowing	−0.0026[a]	−0.0024[a]	−0.0021[a]	−0.0025[a]	−0.0038[a]	−0.0024[a]	−0.0002[b]

The parameters with bold font are the sensitivity parameters.
[a] The sensitivity index of soil N storage on the grazing.
[b] The sensitivity index of soil N storage on the cutting.

where V is the change rate of NDVI, and $NDVI_{max}$ and $NDVI_{min}$ are the maximum and minimum values of NDVI, respectively, in the same pixel from July to August.

The sheep units were calculated (Yu et al., 2010) based on the number of heads of livestock recorded in the statistical yearbook of the Xilingol League (1990–2011) in June in Abag Banner, Xilin Hot, West Ujimqin Banner, and East Ujimqin Banner. The grazing intensity of the study area can be obtained with Eq. 2 based on the grazing steppe area of each administrative region and annual sheep units.

$$GI = \frac{SU}{GA}, \tag{2}$$

where GI is the grazing intensity (heads ha^{-1}); SU is the sheep units (heads); GA is the grazing area (ha).

According to the field survey, the stubble height in the study area varied between 5 and 8 cm, and the height of the dominant species ranged from 60 cm to 80 cm. Therefore, we set the mowing coefficient to 0.75, indicating that the aboveground biomass after mowing was 25% of that before mowing.

2.2.6. Uncertainty analysis method

The uncertainties in up-scaling soil N storage estimation come mainly from the spatial heterogeneity of input parameters of the DNDC model. To bring the uncertainty under control for DNDC, Li et al. (2004) developed the most sensitive factor (MSF) method. According to the approach, the DNDC model was run twice for each simulation unit with the maximum and minimum values of the most sensitive soil factors commonly observed in the simulation unit. The simulated two values formed a range, which was wide enough to include the “real” value from the simulation unit with a high probability.

In this study, the sensitivity of modeled soil N storage on variations in input parameters was determined with the sensitivity index method (Friend et al., 1993; Werner et al., 2007). The variation range was set to ± 20% of the baseline value of a given parameter except the bulk density, which was set to ± 10% of the baseline value because it has a lower standard deviation ratio than other parameters. The mean of the increasing sensitivity index and decreasing sensitivity index of a given parameter was taken as the final sensitivity index. The sensitivity index was calculated as follows

$$\beta = \frac{\left[\frac{(SN_l)-(SN_0)}{SN_0}\right]}{\left[\frac{(P_l-P_0)}{P_0}\right]}$$

where β is the sensitivity index; SN_l is the soil N storage level with the maximum or minimum of a sensitivity parameter; SN_0 is the soil N storage with initial value of a sensitivity parameter; P_l is the maximum or minimum of the sensitivity parameter; P_0 is the initial value of the sensitivity parameter. If the β is positive, the soil N storage and a given parameter change toward the same direction, whereas they change toward two opposite directions otherwise. For a given parameter, the greater the absolute value of β is, the more sensitive soil N storage is. If β is 0, a given parameter has no effect on soil N storage.

To weaken the effect of the vegetation type difference on the sensitivity of soil N storage on input parameters, the sensitivity index of each vegetation type was calculated. The main input parameters and the sensitivity indexes of different vegetation type steppes are listed in Table 3. SOC, Bulk density, N fixation index, and pH were selected as the most sensitivity factors. The variation range of SOC was determined with the maximum and minimum in the same soil type using the soil survey database, and the bulk density and pH were determined with the soil samples of the same soil type. The variation range of SOC, bulk density and pH are listed in Table 2. The minimum of the N fixation index is 1, which assumes that the vegetation had no N fixation. Kang et al. (2011) obtained a N fixation index of 1.5 in a *Leymus chinensis* steppe site, which has been fenced off for more than 25 years. Based on the field vegetation investigation, the grazed steppe generally has fewer nitrogen-fixing plants than the fenced steppe without grazing. Therefore, we took the 1.5 as the maximum of the N fixing index of the study area and determined that the range of N fixing index is between 1 and 1.5. When modeling soil N storage in the typical steppe ecosystem, we selected the minimum SOC content, minimum bulk density, minimum N fixation index, and maximum pH to form a scenario for the DNDC model, which is assumed to produce a low value of soil N storage for a simulation unit, and then selected the maximum SOC content, maximum bulk density, maximum N fixation index, and minimum pH to form another scenario, which is assumed to produce a high value of soil N storage for the simulation unit. Thus, the DNDC model will run twice with the two scenarios for each simulation unit to produce two values. The two values will form a range, which is assumed to be wide enough to cover the “real” value with a high probability.

3. Results

3.1. Temporal-spatial variation in soil N storage

Fig. 3A to Fig. 4C illustrate the spatial distribution of soil N storage from 1990 to 2011. The area with high soil N storage (high-N area), which accounts for 7.65% of the whole study area, is mainly in the east. The area with medium soil N storage (medium-N area), which accounts for 65.07% of the whole study area, is mainly in the middle. The area with low soil N storage (low-N area), which accounts for 27.28% of the whole study area, is mainly located in the west and partly in the middle. The spatial pattern of soil N storage does not change much throughout the region from 1990 to 2011.

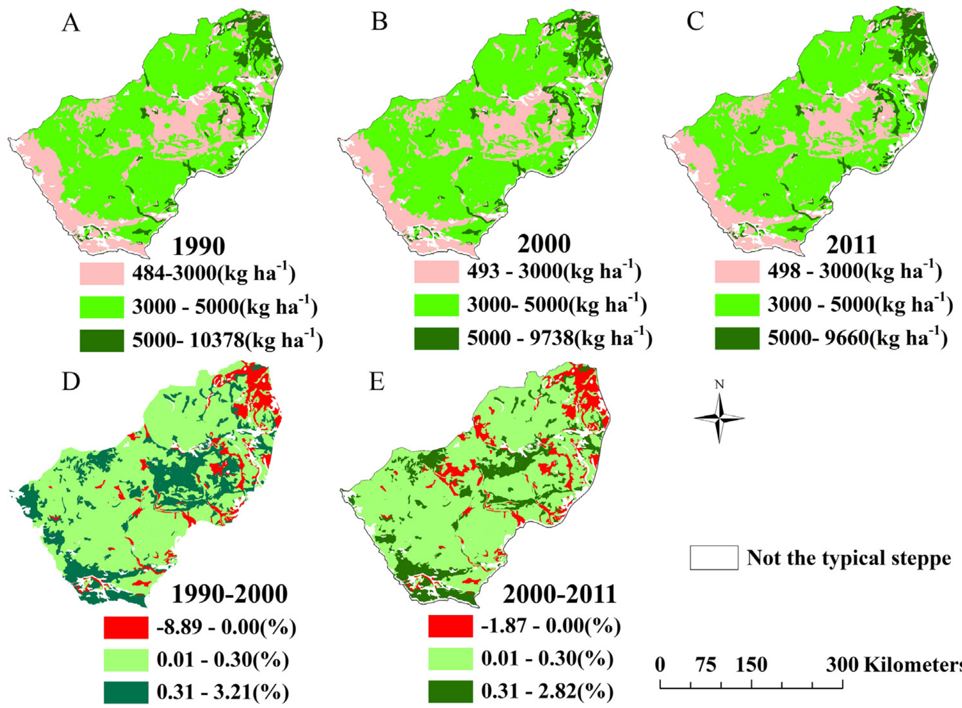

Fig. 3. Spatial distribution (A–C) (kg ha^{-1}) and variation rate (D and E) (%) of soil N storage.

Variation in soil N storage mainly occurred in the high-N and low-N areas (Fig. 3D and E). At a temporal pattern, the soil N storage increased in the low-N area, and the growth rate varied between 0.31 and 3.21% from 1990 to 2000 and between 0.31 and 2.82% from 2000 to 2011. By contrast, the soil N storage decreased in the high-N area, and the growth rate varied between −8.89 and 0% from 1990 to 2000 and between −1.87 and 0% from 2000 to 2011.

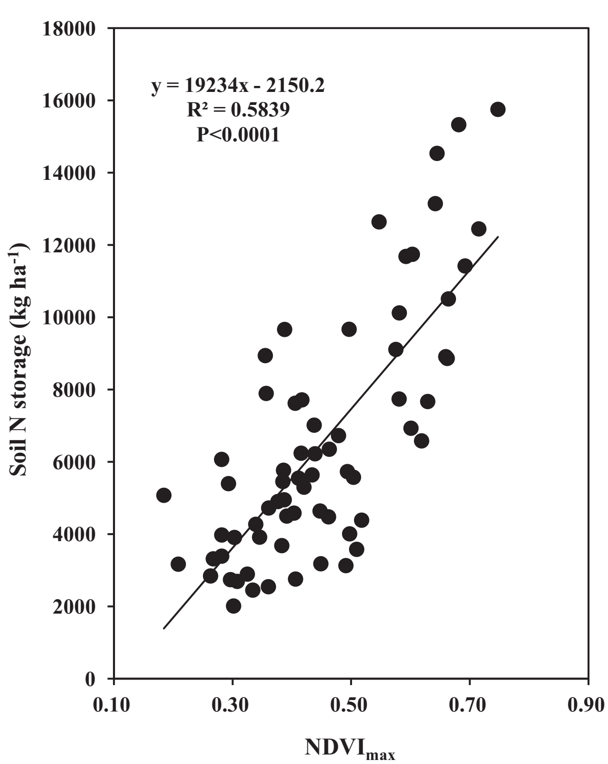

Fig. 4. Pixel-level regression between $NDVI_{max}$ and soil N storage.

3.2. Result comparison

The quantitative measurement of the rationality of the simulation of a large temporal-spatial scale is difficult because of insufficient historical verification data. With a significant regression relation between $NDVI_{max}$ and the observed soil N storage in 2011(Fig. 4), the remote sensing inversion values of soil N storage can be obtained, which provided a comparable result for the simulation soil N storage with the DNDC model. Quantitative evaluation of the rationality of the results was performed using the correlation coefficient (r), root mean square error (RMSE), and relative root mean square error (RMSE%). There is a significant correlation ($P < 0.01$) between the soil N storage obtained by remote sensing inversion and that simulated with DNDC in 1990, 1994, 1998, 2002, and 2006, with 45 verification points extracted randomly at the pixel level (Fig. 5). The correlation coefficients (r) in all years were greater than 0.5, except in 1998. The RMSE did not exceed 2000 kg ha^{-1}, and the RMSE% did not exceed 40% with all verification points, except in 2002 and 2010. Thirty verification points were extracted, with an RMSE between 548.64 kg ha^{-1} and 1078.75 kg ha^{-1} and RMSE(%) between 14.97 and 22.36% in all years. These results suggest that DNDC simulation matches well with those of obtained with remote sensing inversion.

3.3. Uncertainty of results

There was a large difference between the simulated soil N storage with the upper value and that with the lower value of sensitivity parameters. The mean soil N storage simulated with the DNDC model varied from 2339.61 to 5484.61 kg ha^{-1}, and the mean difference was 3145 kg ha^{-1} from 1990 to 2011. Furthermore, when the sensitivity parameters change from the upper value to the lower value, there was a trend change. There was opposite trend between the soil N storage simulated with the upper value and with the lower value. The former has an approximate linear upward trend, whereas the later has an approximate linear downward trend between 1990 and 2011. The simulated soil N storage with the baseline value decreased before 2001 year and then increased slowly (Fig. 6).

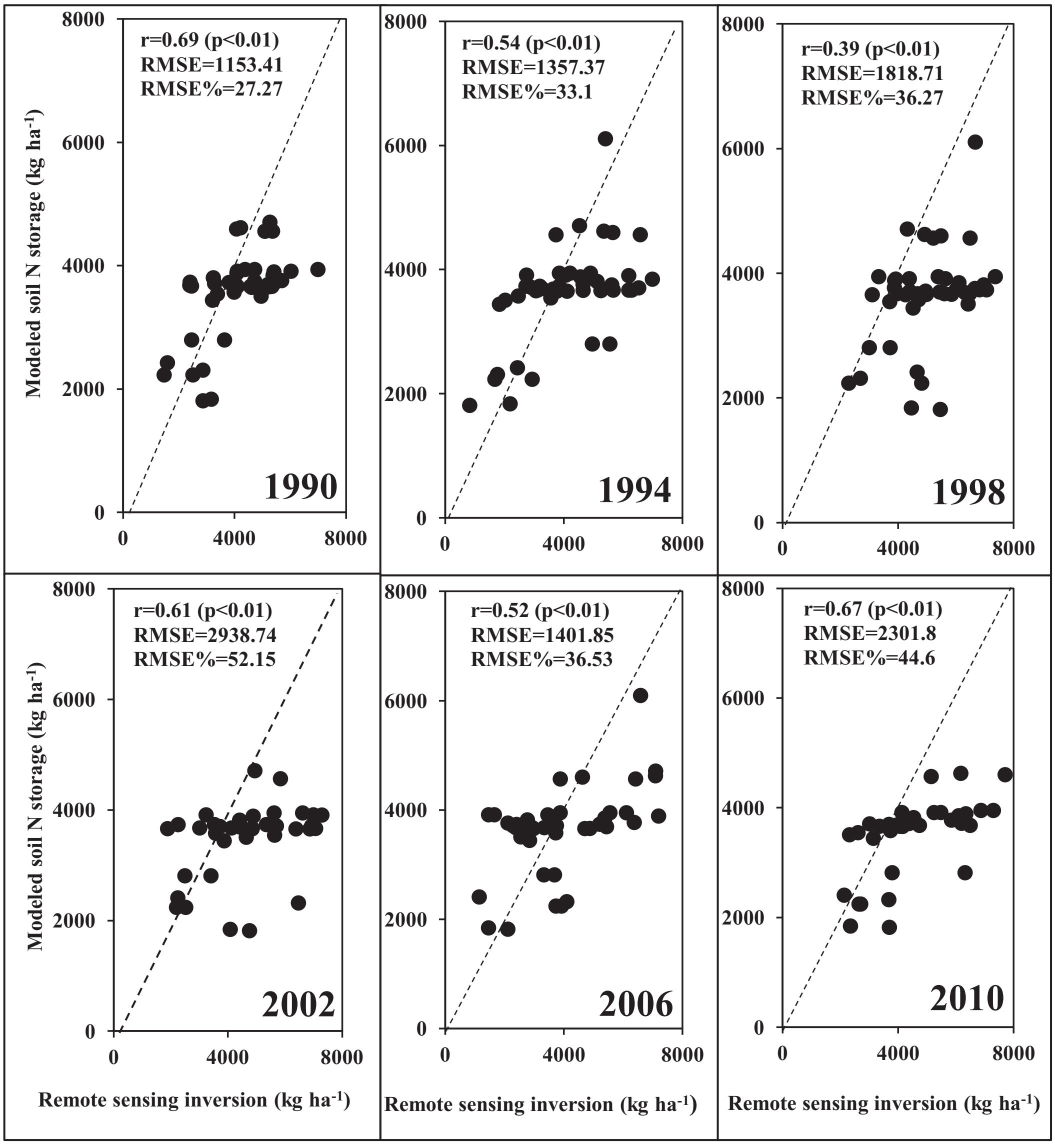

Fig. 5. Comparison of soil N storage obtained by remote sensing inversion with that simulated with the DNDC model.

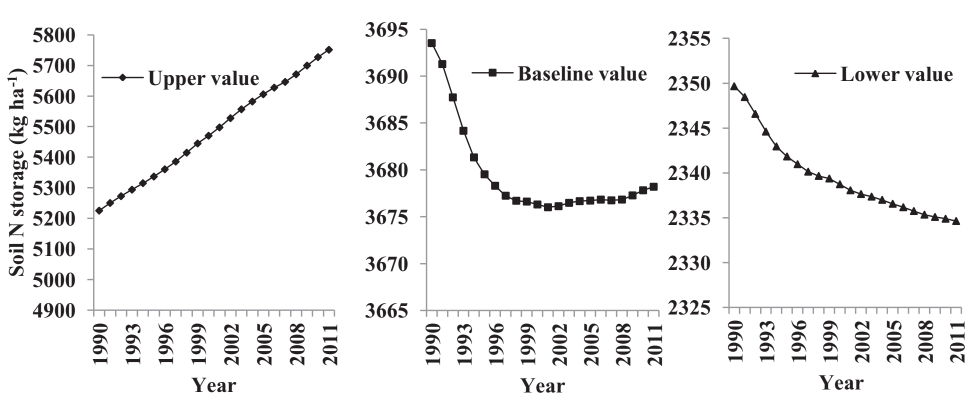

Fig. 6. Annual mean of soil N storage simulated with the upper value, baseline value and lower value of the most sensitivity parameters throughout the study area from 1990 to 2011.

4. Discussion

Steppe ecosystem degradation is a major pressure on sustainable ecosystem development in the arid and semi-arid areas throughout the world (Reynolds et al., 2007). The simulation of soil N storage is of significance to monitoring steppe degradation and make countermeasures. This study provided a simulation framework at the regional scale by integrating the DNDC model and multi-source remote sensing data through a case study in the typical steppe of Xilingol League of Inner Mongolia, China. In this framework, soil N storage was calculated with the biogeochemical processes of N turnover in the DNDC, and remote sensing data were input into the DNDC model as driving factors. Simulation results provide an important reference for steppe management, and the simulation framework can be applied to other similar areas.

Soil N storage declined from the east to west in the study area in this work, which is in accord with the rainfall distribution of the region. The relation between soil N storage, and rainfall was previously confirmed by Abreu et al. (2011). This association can be attributed to the fact that the study area is a steppe under natural conditions in a semi-arid region of China. Rainfall is a main limiting factor in vegetative growth and one of key factors controlling the rate of the decomposition of organic matter (Li et al., 1992). The nutrients of the steppe under natural conditions mainly come from decomposing litter. Therefore, in the study area, the more rainfall there is, the better vegetation grows, and the more vegetation roots in the soil and the soil surface litter there are, the more soil organic matter and soil N storage are produced (Liu et al., 2006). The corresponding order of soil N storage in zonal soil types was light chernozem > meadow chestnut > dark chestnut > chestnut > light chestnut from east to west in the study area. This result is agreement with the results of Tian et al. (2006) and Yang et al. (2007) for the soil N storage of different soil types in China.

Although this study demonstrated the feasibility of monitoring temporal-spatial variation of soil N storage by integration of the DNDC model and remote sensing data, some uncertainty still remains to be addressed. Input parameters and scale are the main factors affecting the uncertainty of the simulation results (Wang and Chen, 2012). According to the uncertainty analysis, SOC, bulk density, pH, and the N fixation index are the most sensitive parameters. SOC is a sensitivity parameter for carbon sequestration (Li et al., 2004), and C and N move through terrestrial ecosystems in coupled biogeochemical cycles (Li et al., 2005). Therefore, the variation of SOC have an impact on the soil N storage. Bulk and pH are the sensitivity parameters of N_2O emission because of their effects on nitrification and denitrification (Kiese et al., 2005; Werner et al., 2007). Nitrification and nitrification are the main soil N biochemical process, in which the organic N can be converted to inorganic N that can be uptaken by plants, and some will be lost to the atmosphere in gaseous form or be leached to the deep soil. Therefore, the sensitivity of soil N storage to the bulk density and pH may be due to the effects of bulk density and pH on nitrification and denitrification. The pronounced sensitivity of soil N storage to the N fixation index is due to the fact the N fixation of vegetation is the main N input for the natural steppe. In the long term, the sensitivity parameters could affect the change tendency of mean soil N storage as well as the level of mean soil N storage throughout the study area (Fig. 6). However, the SOC, pH, soil bulk density and other soil parameters were determined according to the soil type profile data, and the vegetation N fixation index and other vegetation parameters were determined according to the default value of DNDC or the quadrat survey at the sample spot scale. These input parameters introduce uncertainty for the upscaling of the spatial scale (Giltrap et al., 2010; Heuvelink, 1998).

Rainfall, temperature, and grazing or mowing were not the sensitivity parameters of soil N storage. There might be a lag response of soil N storage to the variation of these parameters. At a large temporal-spatial scale, there may be a pronounced impact on the soil N storage. Therefore, these parameters may also introduce uncertainty to the simulation results. Furthermore, the study area is between the meadow steppe and the desert grassland, and the climate transition characteristics are important. Rainfall and temperature diminish from southeast to northwest. For the simulation units far from a weather station, the actual weather might be different from the input climate data and might show more uncertainty than near the weather station. In addition, grazing intensity was determined according to the ratio between the livestock amount and grazing area recorded by relevant banners (county). In fact, grazing intensity is closely related to the residential location of the herdsmen, location of water source, and grazing route (Wang et al., 2012). Taking the average grazing intensity as the regional grazing intensity may increase the uncertainty of the simulation results. The mowing coefficient was determined according to the stubble amount obtained in the sample plot survey. The stubble amount is influenced by landform and stone particle amount in the land surface. Thus, the uniform mowing coefficient may affect the accuracy of the simulation result. In addition, the grazing and mowing regions, which were separated with the change rate of NDVI in the study area from July to August, may be influenced by the intensity of human activities in the region. For a pasture with a rotational grazing system, a grazing region with too much livestock in a short period may be wrongly classified as a mowing region, and a mowing region with a comparatively high stubble may also be wrongly classified as a grazing region. Incorrect grazing and mowing parameters lead to a deviation in simulation results.

There are still limitations of the simulation framework of the DNDC model supported by remote sensing. The temporal-spatial scale is different between the resolution of remote-sensed imagery and the simulation units, which may influence the accuracy of input parameters and the verification of the results (Giltrap et al., 2010; Li et al., 2011). For example, the annual rainfall anomalies may have an important effect on the remote sensing inversion of soil N storage but have little effect on the simulation results. The match between the soil N storage determined by remote sensing inversion and that simulated with DNDC was poorer in 1998, 2002 and 2010 than in other years (Fig. 5). The reason might be rainfall anomalies in those three years. The large difference in spatial scale between the simulation unit and the resolution of remote sensing imagery may have effect on the match between the simulation of soil N storage and that determined by remote sensing inversion. In summary, the simulation of soil N storage on the regional scale is feasible with the DNDC model supported by remote sensing, but there is still much uncertainty that requires systematic analysis in future work to resolve.

5. Conclusions

Soil N storage is an important indicator for monitoring steppe degradation. In this research, the DNDC model supported by remotely sensed parameters was tested for soil N storage simulation, and the simulation results were comparable to the data obtained by remote sensing inversion. The soil N storage decreased in the low-N area and increased in the high-N area. The annual mean soil N storage rapidly decreased before the year 2001, and then, the declining trend disappeared, and a slowly increasing trend emerged. The MSF method can be employed to identify the sensitivity parameters of soil N storage variation and determine the range into which the “real” value of soil N storage may fall with a high probability. Thus, the integration of remote sensing and the DNDC model in the simulation of soil N storage variation is feasible.

Acknowledgments

Our research is sponsored by the Major Basic Research Development Program of China (973 Program, Grant No. 2014CB138803), the Key Projects of National Natural Science Foundation of China (41030535), the Free Inquiry Project of State Key Laboratory of Earth Surface Processes and Resource Ecology (2011-TDZY-102), and National Natural Science Foundation of China (41371524). We thank Changsheng Li for his provision of DNDC model. We thank Jianjun Qiu, Liangxin Fan, Ligang Wang, Jia Deng, Hu Li and Zhao Zhang for their assistance in using the DNDC model. We are grateful for the proofreading of Roland Achtziger and the detailed comments of the two anonymous referees.

References

Abreu, S.L., Godsey, C.B., Edwards, J.T., Warren, J.G., 2011. Assessing carbon and nitrogen stocks of no-till systems in Oklahoma. Soil Till. Res. 117, 28–33.

Allison, S.D., Gartner, T.B., Mack, M.C., McGuire, K., Treseder, K., 2010. Nitrogen alters carbon dynamics during early succession in boreal forest. Soil. Biol. Biochem. 42 (7), 1157–1164.

Ammann, C., Spirig, C., Leifeld, J., Neftel, A., 2009. Assessment of the nitrogen and carbon budget of two managed temperate grassland fields. Agr. Ecosyst. Environ. 133 (3–4), 150–162.

Bai, Y.F., Han, X.G., Wu, J., Chen, Z.Z., Li, L.H., 2004. Ecosystem stability and compensatory effects in the Inner Mongolia grassland. Nature 431 (7005), 181–184.

Bai, Y.F., Wu, J., Pan, Q.M., Huang, J.H., Wang, Q.B., Li, F.S., -antuyev, Buy, Han, A., X.G, 2007. Positive linear relationship between productivity and diversity: evidence from the Eurasian Steppe. J. Appl. Ecol. 44 (5), 1023–1034.

Beheydt, D., Boeckx, P., Ahmed, H.P., Cleemput, O.V., 2008. N_2O emission from conventional and minimum-tilled soils. Biol. Fertil. Soils 44, 863–873.

Beheydt, D., Boeckxa, P., Sleutel, S., Li, C.S., Cleemput, O.V., 2007. Validation of DNDC for 22 long-term N_2O field emission measurements. Atmos. Environ. 41, 6196–6211.

Butterbach-Bahl, K., Stange, F., Papen, H., Li, C., 2001. Regional inventory of nitric oxide and nitrous oxide emissions for forest soils of Southeast Germany using the biogeochemical model PnET-N-DNDC. J. Geophys. Res. 106, 34155–34165.

Chen, Z.Z., Wang, S.P., 2000. Chinese typical grassland ecosystem. Science Press, Beijing (in Chinese).

Feng, X.M., Zhao, Y.S., 2011. Grazing intensity monitoring in Northern China steppe: Integrating CENTURY model and MODIS data. Ecol. Indic. 11 (1), 175–182.

Firestone, M.K., Davidson, E.A., 1989. Microbiological basis of NO and N2O production and consumption in soil. In: Andreae, M.O., Schimel, D.S. (Eds.), Exchange of Trace Gases Between Terrestrial Ecosystems and the Atmosphere. John Wiley & Sons, New York, pp. 7–21.

Friend, A.D., Schugart, H.H., Running, S.W., 1993. A physiology-based GAP model of forest dynamics. Ecology 74 (3), 792–797.

Galloway, J.N., Dentener, F.J., Capone, D.G., Boyer, E.W., Howarth, R.W., Seitzinger, S.P., Asner, G.P., Cleveland, C.C., Green, P.A., Holland, E.A., 2004. Nitrogen cycles: past, present, and future. Biogeochemistry 70 (2), 153–226.

Giltrap, D.L., Li, C., Saggar, S., 2010. DNDC: a process-based model of greenhouse gas fluxes from agricultural soils. Agr. Ecosyst. Environ. 136 (3–4), 292–300.

Heuvelink, G.B.M., 1998. Uncertainty analysis in environmental modeling under a change of spatial scale. Nutr. Cycl. Agroecosys. 50, 255–264.

Hilker, T., Lepine, L., Coops, N.C., Jassal, R.S., Black, T.A., Wulder, M.A., Ollinger, S., Tsui, O., Day, M., 2012. Assessing the impact of N-fertilization on biochemical composition and biomass of a Douglas-fir canopy – a remote sensing approach. Agr. Forest Meteorol. 153, 124–133.

Huang, B., Sun, W.X., Zhao, Y.C., 2007. Temporal and spatial variability of soil organic matter and total nitrogen in an agricultural ecosystem as affected by farming practices. Geoderma 139, 336–345.

Jakubauskas, M.E., Legates, D.R., Kastens, J.H., 2001. Harmonic analysis of time-series AVHRR NDVI data. Photogramm. Eng. Rems. 67 (4), 461–470.

Jin, Y.X., Xu, B., Yang, X.C., Li, J.Y., Wang, D.L., Ma, H.L., 2011. Remote sensing dynamic estimation of grass production in Xilinguole, Inner Mongolia. Scientia Sinica Vitae 41 (12), 1185–1195 (in Chinese. with English abstract).

Kang, X., Hao, Y., Li, C., Cui, X., Wang, J., Rui, Y., Niu, H., Wang, Y., 2011. Modeling impacts of climate change on carbon dynamics in a steppe ecosystem in Inner Mongolia, China. J. Soil Sediment 11, 562–576.

Kiese, R., Li, C., Hilbert, D.W., Papen, H., Bahl-Butterbach, K., 2005. Regional application of PnET-N-DNDC for estimating the N_2O source strength of tropical rainforests in the wet tropics of Australia. Global Change Biol. 11 (1), 128–144.

Kirschbaum, M.U.F., Guo, L., Gifford, R.M., 2008. Observed and modelled soil carbon and nitrogen changes after planting a Pinus radiata stand onto former pasture. Soil. Biol. Biochem. 40 (1), 247–257.

Krug, E.C., Winstanley, D., Wang, J., Cardenas, L.M., Misselbrook, T.H., Cuttle, S., Thorman, R.E., Li, C., 2002. The need for comprehensive and consistent treatment of the nitrogen cycle in nitrogen cycling and mass balance studies: I. Terrestrial nitrogen cycle. Sci. Total Environ. 293 (1–3), 1–29.

Li, A., Wu, J., Huang, J., 2012a. Distinguishing between human-induced and climate-driven vegetation changes: a critical application of RESTREND in inner Mongolia. Landscape Ecol. 27 (7), 969–982.

Li, C.S., 2000. Modeling trace gas emissions from agricultural ecosystems. Nutr. Cycl. Agroecosys. 58 (1-3), 259–276.

Li, C.S., Farahbakhshazad, N., Jaynes, D.B., Dinnes, D.L., Salas, W., Laughlin, Mc, D, 2006. Modeling nitrate leaching with a biogeochemical model modified based on observations in a row-crop field in Iowa. Ecol. Model. 196, 116–130.

Li, C.S., Frolking, S., Frolking, T.A., 1992. A model of nitrous-oxide evolution from soil driven by rainfall events:1. model structure and sensitivity. J. Geophys. Res. 97 (D9), 9759–9776.

Li, C.S., Frolking, S., Harriss, R., 1994. Modling carbon biogeochemistry in agricultural soils. Global Biogeochem. Cy. 8 (3), 237–254.

Li, C.S., Frolking, S., Harriss, R., -bahl, Butterbach, K, 2005. Carbon sequestration in arable soils is likely to increase nitrous oxide emissions, offsetting reductions in climate radiative forcing. Climatic Change. 72, 321–338.

Li, C.S., Mosier A, Wassmann R., Cai, Z.C., Zheng, X.H., Huang, Y., Tsuruta, H., Boonjawat, J., Lantin, R., 2004. Modeling greenhouse gas emissions from rice-based production systems: Sensitivity and upscaling. Global Biogeochem. Cy. 18, http://dx.doi.org/10.1029/2003GB002045, GB 1043.

Li, C.S., Salas, W., Zhang, R., Krauter, C., Rotz, A., Mitloehner, F., 2012b. Manure-DNDC: a biogeochemical process model for quantifying greenhouse gas and ammonia emissions from livestock manure systems. Nutr. Cycl. Agroecosys. 93 (2), 163–200.

Li, H., Qiu, J., Wang, L., Yang, L., 2011. Advance in a terrestrial biogeochemical model—DNDC model. Acta Ecol. Sin. 31 (2), 91–96.

Liu, P., Huang, J., Han, X., Osbert, J.S., Zhou, Z., 2006. Differential responses of litter decomposition to increased soil nutrients and water between two contrasting grassland plant species of Inner Mongolia, China. Appl. Soil Ecol. 34 (23), 266–275.

Liu, X.M., Zhang, W.W., Zhang, M.H., Ficklin, D.L., Wang, F., 2009. Spatio-temporal variations of soil nutrients influenced by an altered land tenure system in China. Geoderma. 152, 23–34.

Parton, W.J., Mosier, A.R., Ojima, D.S., Valentine, D.W., Schimel, D.S., Weier, K., Kulmala, A.E., 1996. Generalized model for N_2 and N_2O production from nitrification and denitrification. Global Biogeochem. Cy. 10 (3), 401–412.

Parton, W.J., Schimel, D.S., Cole, C.V., Ojima, D.S., 1987. Analysis of factors controlling soil organic matter levels in Great Plains grasslands. Soil Sci. Soc. of Am. J. 51 (5), 1173–1179.

Potter, C.S., Randerson, J.T., Field, C.B., 1993. Terrestrial ecosystem production: A process Global Biogeochem model based on global satellite and surface data. Global Biogeochem. Cy. 7 (4), 811–841.

Qi, Z., Bartling, P.N.S., Ahuja, L.R., Derner, J.D., Dunn, G.H., Ma, L., 2012. Development and evaluation of the carbon nitrogen cycle module for the GPFARM-Range model. Comput. Electron. Agr. 83, 1–10.

Reynolds, J.F., Stafford Smith, D.M., Lambin, E.F., Turner, B.L., Mortimore, M., Batterbury, S.P.J., Downing, T.E., Dowlatabadi, H., Fernandez, R.J., Herrick, J.E., Huber-Sannwald, E., Jiang, H., Leemans, R., Lynam, T., Maestre, F.T., Ayarza, M., Walker, B., 2007. Global desertification: building a science for dry-land development. Science 316 (5826), 847–851.

Ryu, C., Suguri, M., Umeda, M., 2011. Multivariate analysis of nitrogen content for rice at the heading stage using reflectance of airborne hyperspectral remote sensing. Field Crop Res. 122 (3), 214–224.

Soil Fertilizer Workstation of Xilingol League, 1989. Soil of Xilingol League. Inner Mongolia people's Press, Hohhot City.

Tian, H.Q., Wang, S.Q., Liu, J.Y., Pan, S.F., Chen, H., Zhang, C., Shi, X.Z., 2006. Patterns of soil nitrogen storage in China. Global Bilgeochem. Cy. 20, 1–9.

Verdoodt, A., Mureithi, S.M., Ye, L.M., Van Ranst, E., 2009. Chronosequence analysis of two enclosure management strategies in degraded rangeland of semi-arid Kenya. Agr. Ecosyst. Environ. 129 (1-3), 332–339.

Veum, K.S., Goyne, K.W., Holan, S.H., Motavalli, P.P., 2011. Assessment of soil organic carbon and total nitrogen under conservation management practices in the Central Claypan Region, Missouri, USA. Geoderma 167-168, 188–196.

Wang, G., Chen, S., 2012. A review on parameterization and uncertainty in modeling greenhouse gas emissions from soil. Geoderma 170, 206–216.

Wang, J., Cardenas, L.M., Misselbrook, T.H., Cuttle, S., Thorman, R., Li, E., C, 2012. Modelling nitrous oxide emissions from grazed grassland systems. Environ. Pollut. 162, 223–233.

Wang, S., Wilkes, A., Zhang, Z., Chang, X., Lang, R., Wang, Y., Niu, H., 2011. Management and land use change effects on soil carbon in northern China's grasslands: a synthesis. Agr. Ecosyst. Environ. 142 (3-4), 329–340.

Wang, Y.H., Zhou, G.S., Wang, Y.L., 2007. Modeling responses of the meadow steppe dominated by Leymus chinensis to climate change. Climatic Change 82 (3-4), 437–452.

Wang, Y.P., Meyer, C.P., Galbally, I.E., 1997. Comparisons of field measurements of carbon dioxide and nitrous oxide fluxes with model simulations for a legume pasture in southeast Australia. J. Geophys. Res. 102, 28013–28024.

Werner, C., Butterbach-Bahl, Haas Hickler, T.K.E., Kiese, R., 2007. A global inventory of N_2O emissions from tropical rainforest soils using a detailed biogeochemical model. Global Biogeochem. Cy., http://dx.doi.org/10.1029/2006GB002909.

Wu, J., Loucks, O.L., 1992. Xilingele (The Xilingol Grassland). In: The National Research Council, U.S. (Ed.), Grasslands and grassland sciences in Northern China. National Academy Press, Washington, DC, pp. 67–84.

Xu, R., Wang, M., Wang, Y., 2003. Using a modified DNDC model to estimate N_2O fluxes from semi-arid grassland in China. Soil. Biol. Biochem. 35 (4), 615–620.

Yang, Y.H., Ma, W.H., Mohammat, A., Fang, J.Y., 2007. Storage, Patterns and Controls of Soil Nitrogen in China. Pedosphere 17 (6), 776–785.

Yu, L., Zhou, L., Liu, W., Zhou, H.K., 2010. Using remote sensing and GIS technologies to estimate grass yield and livestock carrying capacity of alpine grasslands in Golog Prefecture, China. Pedosphere 20 (3), 342–351.

Yu, Z.Y., Zeng, D.H., Jang, F.Q., Fan, Z.P., Chen, F.S., Zhao, Q., 2006. Responses of key carbon cycling processes to the addition of water and fertilizers to sandy grassland in semi-arid region. J. Beijing Forestry University 28 (4), 45–50 (in Chinese, with English abstract).

Zhou, X., Zhang, Y., Ji, X., Downing, A., Serpe, M., 2011. Combined effects of nitrogen deposition and water stress on growth and physiological responses of two annual desert plants in northwestern China. Environ. Exp. Bot. 74, 1–8.